Full wave function cloning for improving convergence of the multiconfigurational Ehrenfest method: Tests in the zero-temperature spin-boson model regime

Special Collection: Algorithms and Software for Open Quantum System Dynamics

Ryan Brook ; Christopher Symonds ; Dmitrii V. Shalashilin ✉

Check for updates

View Online

Export Citation

The Journal of Chemical Physics

Special Topic: Molecular Dynamics, Methods and Applications 60 Years after Rahman

Submit Today

AIP Publishing

AIP Publishing

Full wave function cloning for improving convergence of the multiconfigurational Ehrenfest method: Tests in the zero-temperature spin-boson model regime

View Online   Export Citation   CrossMark

Ryan Brook,[1] (iD) Christopher Symonds,[2] (iD) and Dmitrii V. Shalashilin[1,a] (iD)

AFFILIATIONS

[1] School of Chemistry, University of Leeds, Leeds LS2 9JT, United Kingdom
[2] Fujitsu Services, Lovelace Road, Bracknell RG12 8SN, United Kingdom

Note: This paper is part of the JCP Special Topic on Algorithms and Software for Open Quantum System Dynamics.
[a] Author to whom correspondence should be addressed: d.shalashilin@leeds.ac.uk

ABSTRACT

In this paper, we report a new algorithm for creating an adaptive basis set in the Multiconfigurational Ehrenfest (MCE) method, which is termed Full Cloning (FC), and test it together with the existing Multiple Cloning (MC) using the spin-boson model at zero-temperature as a benchmark. The zero-temperature spin-boson regime is a common hurdle in the development of methods that seek to model quantum dynamics. Two versions of MCE exist. We demonstrate that MC is vital for the convergence of MCE version 2 (MCEv2). The first version (MCEv1) converges much better than MCEv2, but FC improves its convergence in a few cases where it is hard to converge it with the help of a reasonably small size of the basis set.

I. INTRODUCTION

Multidimensional model systems often serve as testing grounds for quantum dynamical methods that aim to circumvent the infamous "curse of dimensionality." Arguably, the most famous model is the Spin-Boson Model (SBM),[1] where two potential surfaces of two distinct quantum states are coupled to a bosonic bath, which can be used to represent a rather wide range of phenomena.[2–8] The SBM can be used to model many different scenarios in multiple fields. In computational chemistry, the SBM is often thought of as a two-state electronic "system" coupled to a continuous "bath" of nuclear vibrational degrees of freedom, and we shall be using this physical picture throughout this article. Within this picture, it is natural to discretize the spectrum of the bath and represent it as a large but still finite number of vibrational modes. A wide range of methods have been developed, which can simulate quantum dynamics of the SBM. Among them are the techniques based on approximations, such as semiclassical approximations[9–12] or fully

quantum approaches.[13–17] However, exact quantum methods are difficult to converge for high dimensional systems or systems outside of their ideal parameters. The zero-temperature regime is arguably the most difficult to simulate, due to the domination of quantum effects and the high number of modes required for accurate simulation. It acts as a convergence limit for several methods,[13] and in the case of certain methods such as the hierarchical equations of motion, new extensions have been created to surpass that limitation,[18–20] albeit with greater computational costs.[21] The multiconfigurational time-dependent Hartree method (MCTDH)[22] and its multilayer extension[23] have both demonstrated their efficiency for the simulations of quantum dynamics of the SBM. MCTDH can converge a wide range of parameters within this regime,[24–26] presenting results for both weak and strong couplings across multiple characteristic frequencies. This method uses a basis set of single particle functions to represent the wave function and to accurately treat high dimensional systems. The bath of the system is handled by a grouping of the different modes such that a small amount of flexible and

30 August 2024 10:51:38

complicated time-dependent linear combinations of single particle functions can handle a significant number of degrees of freedom. This grouping needs to be done correctly to maintain the method's efficiency and its ability to converge at a reasonable cost.

Previously, our group presented the Multiconfigurational Ehrenfest (MCE) approach, a collection of two methods, called version 1 (see Ref. 27) and version 2 (see Ref. 28) (shortened to MCEv1 and MCEv2 for ease). Both MCEv1 and MCEv2 use time-dependent basis functions called Ehrenfest configurations to exactly represent the full quantum system. Our approach belongs to the family of methods based upon the use of trajectory-guided frozen Coherent States (CSs) to describe nuclear motion. The use of the frozen Gaussian coherent states, originally proposed by Heller in 1981,[29] allows for an economically small basis set that is capable of accurately following the quantum system. However, the general idea of using multiple Gaussians can be traced back to 1973 when Shore and Sander simulated coupled Einstein phonons with two Gaussians.[30] The main difference between coherent state based methods is then in the choice of trajectory that is used to guide the basis set. Classical trajectories are the cheapest and the simplest, allowing for methods such as multiple spawning[31–34] to produce results rapidly. However, these classical trajectories, while being advantageous in terms of computational time, are prohibited from accessing non-classical space and therefore sometimes fail to capture quantum effects. This causes the method to struggle to treat systems described as "highly quantum" such as the presently considered zero-temperature cases. If the trajectories are chosen to be entirely quantum and variational, such as in the Variational Multiconfigurational Gaussians (vMCG),[35] the trajectories often accurately follow the quantum wave function, but, numerically, vMCG is difficult and expensive. These disadvantages impose a limit to the dimensionality of the systems that can be treated, meaning that methods such as these cannot access the spin-boson systems with a high number of bath modes. The Ehrenfest trajectories employed by MCE represent a compromise between the simplicity of classical dynamics and the accuracy of variational methods. The quantum nature of the trajectories allows them to capture quantum effects while remaining relatively computationally inexpensive. Although MCEv1 and MCEv2 use the same Ehrenfest trajectories to guide nuclear motion (bath), they differ by the dynamics of electronic amplitudes (system) and use different wave function *Ansätze*. In MCEv2, only the amplitudes within the same Ehrenfest configuration are coupled, making the trajectories independent. In MCEv1, the trajectories are more complicated as their electronic state amplitudes are coupled across the trajectories, and therefore, the trajectories interact with each other.

It is also important to note that MCEv1 shares a functionally identical *Ansatz* with the multi-D_2 Davydov trail states,[36] one of the two multiple Davydov *Ansätze* (mDA). The mDA are themselves a subset of the hierarchy of Davydov's *Ansatz* (hDa), with the original idea of Davydov's soliton originating in the 1970s.[37,38] The hDa methods are extensive, for example after momentum-space projection, the Davydov D_2 results in Toyozawa's *Ansatz*.[39–41] The different Davydov *Ansätze* have been applied to the SBM across many regimes with notable success.[17,42,43] The difference between the two methods lies in the fact that while the equations of motion for mDA are purely variational, MCE relies on Ehrenfest trajectories to propagate the nuclear part of the basis set on a mean field. The direct consequences of the different choice for the equations

of motion are visible when MCEv1 was directly compared against the multi-D_2 *Ansatz* when MCEv1 was extended to investigate the dynamics of a one-dimensional Holstein molecular crystal model,[44] where both methods were found to be in great agreement with the benchmark HEOM for small transfer integrals. For all cases considered, the multiplicity of the multi-D_2 *Ansatz* ranged from 32 to 56, where the number of configurations for MCEv1 ranged from the high hundreds to thousands. This stark difference in multiplicity demonstrates how relying on a quantum averaged potential instead of fully variational equations requires a much larger basis set. However, when approaching larger transfer integrals, beyond the computational limitations of HEOM, MCEv1 was able to increase the number of configurations into the thousands and was shown to be able to converge to the correct dynamical properties of the Holstein polaron for large transfer integral. As noted in a recent perspective on the hierarchy of Davydov *Ansätze*,[45] the likeness of MCE and mDA allows for fairly straightforward transfer of ideas and frameworks between such methods.

The convergence of trajectory-guided CS-based methods crucially depends on the sampling of initial conditions of trajectories and on several adaptive basis set recipes that make the basis set follow quantum dynamics more efficiently. In this paper, we develop further the idea of basis set cloning, a technique that helps describe the effect of wave packet splitting. The original iteration of cloning, called Multiple Cloning (MC), intends to correct potential misguiding of the basis set when the Ehrenfest trajectories may not hold to be a faithful representation of the path of the system. Cloning has been successfully implemented in MCEv2, where an extra basis function is created from a misguided basis function after its trajectory passes the region of the nonadiabatic coupling. These created coherent states are identical in phase space and are differentiated only in the way that the contribution from each electronic state (2 in the case of the spin-boson model) is unique to each clone. Every cloning event increases the basis set size by 1. This procedure can then be repeated later in the propagation if the clones themselves are misguided. The cloning technique in MCEv2 had initial success in the *ab initio* version of the method (AIMC)[46–52] and later was applied to the SBM[53] where it was shown that this procedure of growing the basis set by cloning may improve greatly the convergence of MCEv2. The idea of cloning was directly inspired by the spawning procedure implemented in *ab initio* multiple spawning (AIMS),[31,33,34] and was developed to be an analog with AIMC and AIMS being presented as complementary approaches in the original paper of AIMC,[48] and AIMC was run on a modified version of the AIMS-MOLPRO package[54] before being officially added to NWChem[51] and NEXMD v2.0.[55] AIMC can be seen as a halfway point between AIMS and the fully quantum-based methods such as vMCG or mDA, as it combines the best features of both sets of methods, relatively "cheap" trajectories due to Ehrenfest equations of motion propagating the basis set without having to resort to computationally expensive or numerically unstable techniques. The averaged mean-field potential energy surface used in AIMC, however, also contains quantum information, and so, in principle, AIMC is a fully formally exact quantum method. AIMC was shown to agree with AIMS in the simulation of conjugated molecules,[48] and, recently, AIMC has been applied to the simulation of electron excitation.[56] This area of electronic excitation presents a challenge to AIMS as it requires consistent spawning events to maintain coupling

between electronic states, an issue bypassed by AIMC as coupling between the electronic states is included via the construction of the Ehrenfest configuration.

In this paper, we will develop a cloning procedure for MCEv1, for which the coupled Ehrenfest trajectories present an interesting situation. The "push" experienced between the trajectories in MCEv1 is advantageous as the trajectories spread out less and there are some quantum forces between the trajectories included by construction, which keep trajectories in the nonclassical regions. This advantage allows MCEv1 to accurately represent the quantum system for longer timeframes. However, the coupling between trajectories comes with certain drawbacks. The first is that all trajectories must be run simultaneously as each trajectory is dependent on the rest, which unlike MCEv2 makes MCEv1 difficult for the use in direct *ab initio* dynamics. A more notable disadvantage concerning cloning in MCEv1 is that due to the trajectories "pushing" one another, two coherent states cannot exist in the same phase space point of nuclear motion, and the existing cloning procedure in MCEv2 creates a coherent state with identical phase space coordinates. To circumvent this issue, we instead clone the entire basis set and generate two uncoupled nuclear basis sets with unique contributions from each electronic state. Then, we propagate them separately before recombining them with the inclusion of cross terms and quantum interferences. Even though this form of cloning is more severe and costly, the coupled trajectories of MCEv1 allow for better scaling into higher dimensional systems and for larger timeframes due to less trajectory dispersion. The fact that MCEv1 remains accurate for longer times also lessens the required number of cloning events. The issue solved by the introduction of cloning is the misguiding of the basis set by the Ehrenfest trajectories which cloning remedies by allowing the basis set to mimic wave function bifurcation. This combined with the flexible nature of the cloning procedure allows for the method to achieve results that cannot be produced by a simple doubling of the initial basis set, such as the simulation of two-peaked spectra,[49,52] whereas MCE even with a large basis set only produces 1 peak. MCEv1 was shown to be capable of converging a wide range of SBM cases, and so, the new version of cloning should be capable of providing paths to convergence for the remaining outlying cases.

II. FORMULATION OF THE MULTICONFIGURATIONAL EHRENFEST METHOD

This paper confines the MCE methods and their equations to two electronic states in order to better represent the spin-boson model,

$$|0\rangle = \left|\phi_0^{\{system\}}\right\rangle, |1\rangle = \left|\phi_1^{\{system\}}\right\rangle \tag{1}$$

although expansion to a generic number of states is possible and straightforward. Both MCEv1 and MCEv2 are foundationally similar in their use of a bath of multidimensional frozen Gaussian coherent states, which is a product of multiple one-dimensional coherent states,

$$|z_n(t)\rangle = \Pi_{m=1,M}\left|z_n^{(m)}(t)\right\rangle \tag{2}$$

where M is the total number of dimensions, i.e., bath degrees of freedom. The label for the coherent state, z, is itself a combination of

real and imaginary parts of its center, representing the parts of phase space (p, q),

$$z_n^{(m)}(t) = \frac{\gamma^{1/2}q_n^{(m)} + i\left(\frac{\gamma^{-1/2}}{\hbar}\right)p_n^{(m)}}{\sqrt{2}}, \tag{3}$$

whereas the whole coherent state is a Gaussian wave packet (in one dimension),

$$\langle x|z\rangle = \left(\frac{\gamma}{\pi}\right)^{1/4} \exp\left(\frac{\gamma}{2}(x-q)^2 + \frac{ip(x-q)}{\hbar} + \frac{ipq}{2\hbar}\right). \tag{4}$$

Here, γ is the width of the envelope applied to the Gaussian wave packet, which is kept constant to construct "Frozen" Gaussians. The wave function *Ansätze* in MCEv1 and MCEv2 are given as

$$|\Psi(t)\rangle_{MCEv1} = \sum_{n=1,N}\left(a_{1n}|1\rangle + a_{0n}|0\rangle\right)|z_n(t)\rangle \tag{5}$$

and

$$|\Psi(t)\rangle_{MCEv2} = \sum_{n=1,N}A_n(t)\left(a_{1n}|1\rangle + a_{0n}|0\rangle\right)|z_n(t)\rangle \tag{6}$$

respectively, where N is the basis set size.

In both versions of MCE, the Ehrenfest trajectories are used to guide the nuclear coherent state basis functions,

$$i\dot{z}_n = \frac{\partial H^{\{Ehr\}}}{\partial z_n^*}, \tag{7}$$

where the Ehrenfest Hamiltonian, H^{Ehr}, is the Hamiltonian averaged over the system configuration n,

$$H^{\{Ehr\}} = \frac{|a_{1n}|^2\langle z_n|\hat{H}_{11}|z_n\rangle + |a_{0n}|^2\langle z_n|\hat{H}_{00}|z_n\rangle + 2\text{Re}\left(a_{0n}^*a_{1n}\langle z_n|\hat{H}_{10}|z_n\rangle\right)}{|a_{1n}|^2 + |a_{0n}|^2}. \tag{8}$$

Equation (8) is written for the case of the SBM with two system electronic states only, but it can easily be written for more system states. Spin-boson model Hamiltonian matrix elements used in this work can be found in Chap. 2.1 of Ref. 1. Also in Ref. 53, the discretization of the continuous SBM spectrum into a final set of vibrational modes is described.

The equations for the amplitudes in MCE can be found in Refs. 27 and 28 for the two versions, respectively. In the diagrams shown in Figs. 1(a) and 1(b), we illustrate the main difference in the structure of equations. In both methods, the full wave function is a combination of individual Ehrenfest configurations,

$$\left|\varphi_n^{Ehr}\right\rangle = \left(a_{1n}|1\rangle + a_{0n}|0\rangle\right)|z_n(t)\rangle, \tag{9}$$

in which nuclear coherent state basis functions are split between electronic states, but MCEv1 and MCEv2 use different coupling schemes between configurations, which are illustrated in Fig. 1. In MCEv1, all amplitudes a_{in} are coupled with each other, both within individual Ehrenfest configurations and across configurations. The trajectories that result from this way of coupling are not independent and "push" each other [see Fig. 1(a)]. In MCEv2, the amplitudes a_{in} are coupled only within individual Ehrenfest configuration n
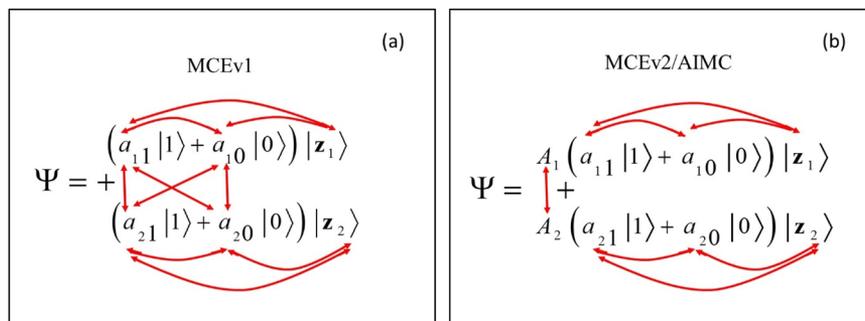
FIG. 1. Coupling between the parameters of the wave function *Ansatz* in (a) MCEv1 and (b) MCEv2. Only two of many coupled basis set configurations are shown.

and the trajectories $z_n(t)$ are independent. In order to account for the quantum coupling between configurations, additional amplitudes $A_n(t)$ are introduced [see Fig. 1(b)]. In MCEv2, configurations (10) are normalized so that for each n, $|a_{1n}|^2 + |a_{0n}|^2 = 1$. This is not the case in MCEv1, where only the whole wave function (6) is normalized.

The independent nature of trajectories in MCEv2 allows for easy use of the method in direct dynamics simulations. In the *Ab Initio* Multiple Cloning (AIMC) method,[48] individual Ehrenfest trajectories are run independently and coupling between their amplitudes $A_n(t)$ is done as post-processing. While independent trajectories are computationally better suited for larger systems, it was found that it is much harder to reach the convergence of MCEv2 than of MCEv1. Nevertheless, independent trajectories are fit for *ab initio* direct dynamics and several tricks that improve the convergence of MCEv2 have been developed. Meanwhile, MCEv1 was found to converge well for many cases of SBM, which means that interacting trajectories follow the quantum wave function much better than independent trajectories of MCEv2.

Running an ensemble of coupled trajectories *ab initio* "on the fly" with MCEv1 is difficult for the moment, but MCEv1 can be used to simulate the dynamics of model systems, where potential energy surfaces are known analytically. Sampling techniques have not been extensively exploited for MCEv1, and in Sec. III, we review the existing MCEv2 sampling tricks and generalize cloning for the use with MCEv1.

III. SAMPLING TECHNIQUES

A. Swarms

Several sampling techniques are greatly important for the timely convergence of the MCE methods.[53,57] Initial coherent states are created as a "swarm," with the distribution shown (10), which is capable of covering the entirety of the initial wave function ($|\Psi_0\rangle = |z_0\rangle$), due to a variable compression parameter, a_c, controlling the size of the Gaussian distribution used to construct the swarm,

$$F(z_n) \propto e^{-a_c|z_n-z_0|^2}. \tag{10}$$

In the cases where certain degrees of freedom can be deemed as more important, it is possible to partition the total bath modes into
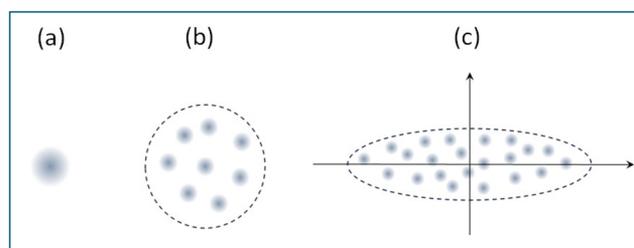

FIG. 2. Graphic showing (a) a singular basis function, (b) a swarm of basic functions within the enclosure governed by the compression parameter a_c, and (c) a pancake of basis functions with a focus on the most important modes.

important and less important modes. Then, by decreasing the compression parameter for the most important modes while increasing the compression parameter for the less important modes, a "pancake" style distribution is created to sample the most relevant modes more accurately [see Fig. 2(c)]. These types of distribution of initial conditions are used for both MCEv1 and MCEv2.

B. Trains

In MCEv2, basis set trains are used in tandem to counteract the decrease in convergence obtained by the introduction of swarms. These trains consist of a "line" of basis functions (see Fig. 3) that are time-shifted along the trajectory, causing the basis set, by construction, to cover a larger area of phase space. This also reduces the randomness of the swarm of coherent states leading to a higher rate of convergence. The space between each of the basis functions forming a given train is controlled by an initial spacing parameter, which can be tuned to a specific system being studied, as the speed at which the basis functions explore the phase space affects the rate at which the basis function trains uncouple.

To form the trains, an initial swarm is generated via continuously increasing the compression parameter until a norm of 1 is achieved, and then for each basis function within that swarm, a train of time-shifted basis functions is created with the train spacing decided by finding the highest separation distance for the basis functions constituting the "carriages" of the train while maintaining the norm. Both of these steps and checks are vital as the norm of the
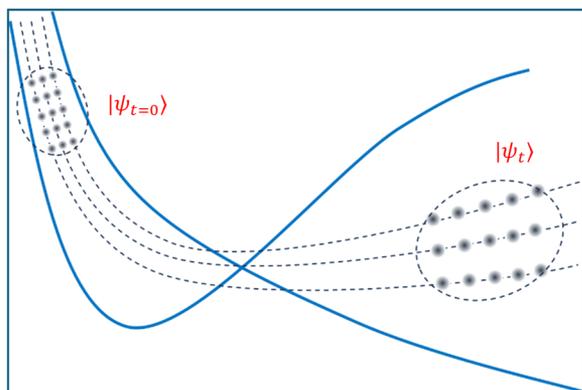
30 August 2024 10:51:38

FIG. 3. A swarm of trains being guided *across potential energy surfaces (blue) through time* via Ehrenfest trajectories (dashed lines). The basis functions within each train follow the same trajectory, reducing the randomness of the swarm and allowing for the reuse of electronic structure information.

basis functions and basis set at large is restricted and must be maintained at 1 due to the inclusion of the additional coupling parameter in MCEv2.

C. Bit-by-bit propagator

A useful tool for the propagation of large basis sets is "bit-by-bit" propagation. If repeat propagations of a smaller basis set are run differing only by the initial conditions, this can effectively mimic the propagation of a larger basis set and allow recovering of the populations of states 1 and 2 via averaging of these many repetitions (see Fig. 4). For the specific case of the spin-boson model, it is apt to
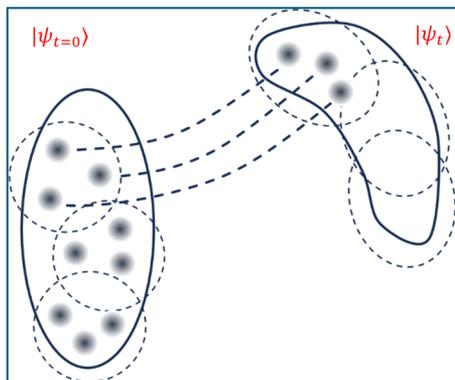

FIG. 4. Coherent state "bits" (the basis functions enclosed by dashed circles) are generated to fully represent the initial wave function. Then, the wave function of each "bit" is represented on a small basis of coherent states and each "bit" is propagated separately. This also shows the strength of trajectory-based methods as the trajectories allow the coherent states to "spotlight" relevant areas of phase space instead of requiring a grid point for every possible coordinate at all times. In this paper, "bits" are sometimes referred to as repeats.

apply this through the harmonic oscillator density operator, $\widehat{\rho}$, of the M coherent states given by

$$\widehat{\rho} = \int |z_{bath}\rangle \rho(z_{bath})\langle z_{bath}| \frac{d^2 z_{bth}}{\pi^M}$$

$$= \prod_{m=1,M} \int |z^{(m)}\rangle \rho(z^{(m)})\langle z^{(m)}| \frac{d^2 z^m}{\pi}, \quad (11)$$

where $d^2 z^{(m)} = \frac{dp^{(m)} dq^{(m)}}{2}$ is phase space integration and z_{bath} is the multidimensional bath coherent state found as a product of all m coherent states representing the M degrees of freedom. For a system of harmonic oscillators, this operator is a product of 1D density operators,

$$\rho\left(z^{(m)}\right) = \sigma^{(m)} e^{-\sigma^{(m)} \left|z^{(m)}\right|^2}. \quad (12)$$

The initial conditions of the "bits" are therefore sampled from a distribution around the "origin" of phase space $(q, p) = (0, 0)$ as shown in Eq. (12). The width of the density matrix, $\sigma^{(m)}$, is controlled by the inverse temperature parameter, β, and the frequency of the bath mode, $\omega^{(m)}$,

$$\sigma^{(m)} = e^{\beta \omega^{(m)}} - 1. \quad (13)$$

In this paper, it is also assumed that initially only the system state $|1\rangle$ is populated. Each "bit" is later propagated using a swarm basis set, as shown in Fig. 4. All "bits" can be propagated in parallel, which makes MCE very efficient. The "bit-by-bit" propagation has been used for both MCEv1 and MCEv2. In this work, we follow the same stratagem, only adding full wave function cloning to MCEv1 as described in Secs. III D and III E.

D. Multiple cloning in MCEv2

A problem suffered by all methods that utilize Ehrenfest trajectories is that of the potential misguiding of the basis once the trajectories enter a region of strong non-adiabatic coupling between electronic states. It is common in these regions for wave functions to undergo bifurcation, causing behavior that can no longer be faithfully represented by the average potential followed by Ehrenfest trajectories. Although, in principle, a very large basis set of Ehrenfest trajectory-guided CSs would converge, in practice, this represents a problem as we want to achieve convergence with the smallest possible basis set size. To rectify this, the computational sampling of cloning is introduced to MCEv2, where an additional basis function is created (see Fig. 5) after entering a region of high coupling and the contribution of the electronic states is split between the two clones,

$$\left|\psi'_n(t)\right\rangle = (A_n|a_{n1}|)\left(\frac{a_{n1}}{|a_{n1}|}|1\rangle + 0|0\rangle\right)|z_n\rangle, \quad (14)$$

$$\left|\psi''_n(t)\right\rangle = (A_n|a_{n0}|)\left(0|1\rangle + \frac{a_{n0}}{|a_{n0}|}|0\rangle\right)|z_n\rangle \quad (15)$$

such that their sum is equal to the contribution of the uncloned function,

$$\left|\psi'_n(t)\right\rangle + \left|\psi''_n(t)\right\rangle = A_n(a_{n1}|1\rangle + a_{n0}|0\rangle)|z_n\rangle \quad (16)$$
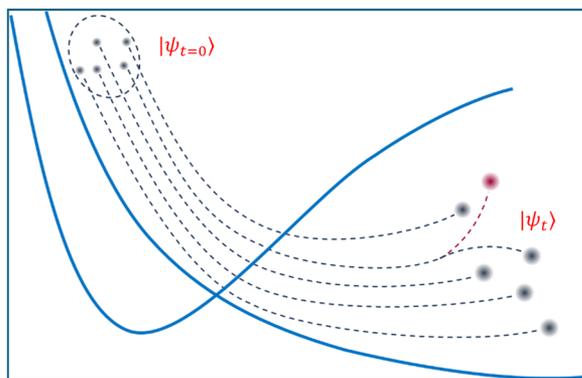
FIG. 5. A swarm of coherent states being guided across potential energy surfaces (blue solid lines) through time via Ehrenfest trajectories (dotted lines). After passing a region of non-adiabatic coupling, only the misguiding trajectories bifurcate, increasing the number of basis functions and allowing the basis set to more accurately capture the entire wave function. In practice, this occurs with trains of swarms. To avoid uncontrollable growth of the basis set, usually a limit of how many times original trajectories can clone is introduced.

In MCEv2, cloning of a basis function is done under certain conditions, which are derived from the analysis of the breaking force, F^{br}, experienced by the configuration, k, from each potential energy surface,

$$F^{br} = |a_{1k}a_{2k}|^2 \nabla (V_1 - V_2). \tag{17}$$

Due to the nature of the potential energy surfaces in the SBM, the differential in their potential remains constant, and therefore, the maximum breaking force is found due to the amplitudes of the configuration only. The theoretical maximum of the breaking force is found when population is split evenly between the two potential energy surfaces and so the simplified condition for cloning for version 2 applied to the SBM is taken to be $\left| a_k^{(1)} a_k^{(2)} \right|^2 > \delta$, where δ has a theoretical maximum of $\frac{1}{4}$ since the amplitudes are normalized for MCEv2. The value of δ can be modified depending on the case studied (see Ref. 53). To avoid uncontrollable explosive growth of the basis set size, usually a limit of how many times original trajectories can clone is introduced.
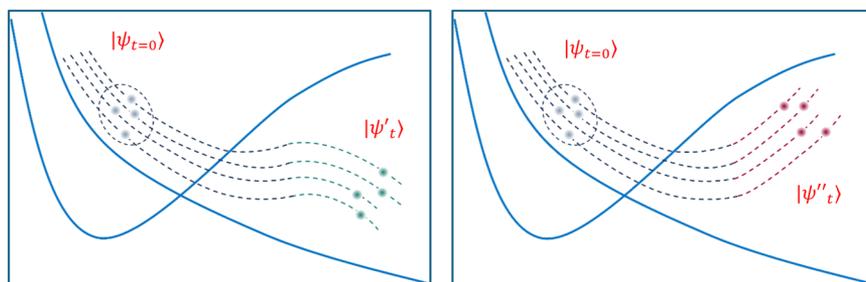
MCEv2 utilizing a combination of all these sampling tricks is often named as Multiple Cloning Multiconfigurational Ehrenfest (MC-MCE) method or *Ab Initio* Multiple Cloning (AIMC) when performing as "on-the-fly" direct dynamics. This paper will refer to MC-MCE as MC-MCEv2 to better differentiate and directly compare the different versions of MCE.

E. Full wave function cloning in MCEv1

The additional amplitude, $A_n(t)$, in the MCEv2 *Ansatz* that separates the inter- and intra-configuration coupling allows for the implementation of cloning on an individual basis function as a consequence of the independent nature of MCEv2 Ehrenfest trajectories. The fact that trajectories "push" each other in MCEv1 due to the inter-configurational coupling between all quantum amplitudes prevents the creation of coherent states in the exact same region of nuclear phase space, disallowing the clones [Eqs. (14) and (15)] used in MCEv2 to be applicable to MCEv1. Instead, we clone the entire wave function as shown in Fig. 6 such that two entire basis sets are created that sum to the original wave function at the time step of cloning,

$$\begin{aligned}
|\Psi(t)\rangle &= \sum_{\{n=1,N\}} (a_{n1}|1\rangle + a_{n0}|0\rangle |z_n(t)\rangle) \\
&= \sum_{\{n=1,N\}} (a_{n1}|1\rangle + 0|0\rangle |z_{n0}{}'(t)\rangle) \\
&\quad + \sum_{\{n=1,N\}} (0|1\rangle + a_{n0}|0\rangle |z_n{}''(t)\rangle. \tag{18}
\end{aligned}$$

Due to the lack of requirement for basis functions to be normalized in MCEv1, it is possible at the time of cloning to assign different initial values for amplitudes as long as the total populations of each electronic state are conserved. A convenient construction for this is through the use of trigonometric functions after random selection of angle θ,

$$\begin{aligned}
|\Psi(t)\rangle &= \sum_{\{n=1,N\}} (a_{n1}|1\rangle + a_{n0}|0\rangle)|z_n(t)\rangle \\
&= \sum_{\{n=1,N\}} (\cos^2(\theta)a_{n1}|1\rangle + \sin^2(\theta)a_{n0}|0\rangle)|z_n{}'(t)\rangle \\
&\quad + \sum_{\{n=1,N\}} (\sin^2(\theta)a_{n1}|1\rangle + \cos^2(\theta)a_{n0}|0\rangle)|z_n{}''(t)\rangle. \tag{19}
\end{aligned}$$

FIG. 6. A swarm of coherent states being guided across potential energy surfaces (blue solid lines) via Ehrenfest trajectories (dashed lines), which are quantum amplitude weighted averages of the potential energy surfaces. After passing a region of non-adiabatic coupling, the trajectories bifurcate, creating two basis sets that are guided along contributions from one potential energy surface initially, representing the rapid swerve of the trajectories toward one of the potential energy surfaces.

While most Full Cloning (FC) in this paper uses Eq. (18), we have experimented with angular cloning with randomly generated θ for some test cases of the SBM.

These two basis sets can then be propagated completely separately with the usual MCEv1 equations of motion, and the cloning procedure can be seen as generating an additional coupled "bit" repeat. This is due to the clones being orthogonal by construction. In a full basis, this orthogonality is maintained throughout propagation. The full cloning procedure simply doubles the computational efforts. However, if we were doubling the initial basis set size, the computational cost would grow much more, as the propagation of two basis sets with n basis functions is significantly computationally cheaper than the propagation of a single basis set with $2n$ basis functions. After propagation is complete, the populations of the overall wave function can be calculated as a post-processing step,

$$P_{\{1,tot\}} = \frac{P_1^{(1)} + P_1^{(2)} + CT_1^{\langle 1|2 \rangle}}{P_1^{(1)} + P_1^{(2)} + P_0^{(1)} + P_0^{(2)} + CT^{\langle 1|2 \rangle}}, \quad (20)$$

$$P_{\{0,tot\}} = \frac{P_0^{(1)} + P_0^{(2)} + CT_1^{\langle 1|2 \rangle}}{P_1^{(1)} + P_1^{(2)} + P_0^{(1)} + P_0^{(2)} + CT^{\langle 1|2 \rangle}}, \quad (21)$$

where the superscript, c, represents the number of the cloned basis set origin and the probabilities $P_i^{(c)}$ are the probabilities of the states $i = 0, 1$ within the clone (c). CT is the cross term between the two cloned basis sets. These cross terms between clones m and l are given by the following equations:

$$CT^{\langle m|l \rangle} = CT_1^{\langle m|l \rangle} + CT_2^{\langle m|l \rangle}, \quad (22)$$

where

$$CT_i^{\langle m|l \rangle} = 2\mathrm{Re}\left(\sum_{kj} a_{ki}^{*(m)} a_{ji}^{(l)} \left\langle z_k^{(m)} | z_j^{(l)} \right\rangle \right). \quad (23)$$

This form of cloning, akin to the cloning in MCEv2, can be repeated to create additional basis sets, albeit with additional cross terms required, but the equations for cross terms between more than 1 set of clones are trivial. However, as with all basis set expansion tricks, excessive cloning events can lead to problematic scaling, as n cloning events require propagation of 2^n basis sets and calculation of $\frac{(2n)!}{(2n-2)!}$ cross terms. This extension of MCEv1 will be referred to as Full Cloning Multiconfigurational Ehrenfest Configurational version 1 (FC-MCEv1). Unlike other aforementioned sampling techniques outlined in this paper, full cloning has never been used and represents the main novel methodological contribution of this paper.

IV. THE SPIN-BOSON MODEL

The SBM is a two-state system coupled to a harmonic bath. In the computational chemistry context, these diabatic donor and acceptor states often represent potential energy surfaces. The Hamiltonian for the SBM is given by

$$\hat{H}_{SBM} = \begin{bmatrix} H_B + H_C + \varepsilon & \Delta \\ \Delta & H_B - H_C - \varepsilon \end{bmatrix}, \quad (24)$$

where ε and Δ are the bias tuning parameter and the tunneling parameter, respectively, and can be taken to be constants for any given specific case of the SBM. The partial Hamiltonians of the bath and coupling, H_B and H_C, contain the frequency of the mode and the coupling between the system and the bath,

$$\hat{H}_B = \sum_m \omega^{(m)}\left(\hat{a}^* \hat{a} + \frac{1}{2} \right), \quad (25)$$

$$\hat{H}_C = \sum_m \frac{C^{(m)}}{\sqrt{2\omega^{(m)}}}\left(\hat{a}^* + \hat{a} \right). \quad (26)$$

Total information about the bath is contained within the spectral density function whose many parameters allow the simulation of many phenomena. This paper reports only on the Ohmic exponential cutoff form of the SBM spectral density that increases linearly with frequency until decaying exponentially after the characteristic frequency, ω_c, is reached. The equation for this form of the spectral density is

$$J(\omega) = \frac{\pi}{2}\alpha_K \omega e^{-\frac{\omega}{\omega_c}}, \quad (27)$$

where α_K is the Kondo parameter, which describes the strength of the coupling between the system and the bath. See Refs. 27 and 53 and, in particular, Ref. 58 where discretization of the SBM was outlined in greater detail.

V. RESULTS

We have used "bit-by-bit" propagation similar to Ref. 53 and simulated several cases of the spin-boson model with both MCEv1 and MCEv2. When necessary to increase convergence, MCEv1 will be run with full cloning [see Eq. (17)] and MCEv2 will run with single basis function multiple cloning [see Eqs. (14) and (15)]. In all cases, even without cloning, MCEv1 is at least semiquantitatively correct, but the newly presented full cloning makes it even better. We have used existing benchmarks, but in Sec. VI of this paper, we discuss the need for an automated way of converging MCEv1 by itself, which would include a condition, or a set of conditions, for automated full cloning, similar to those already developed for MCEv2, and as such FC-MCEv1 is a semi-manual process. Unless explicitly stated, the full cloning condition for the zero-temperature cases considered in this work was taken to be when the population difference was 0.

As has been done previously when introducing new convergence techniques for MCE methods, we consider regimes of the SBM to test the full cloning technique. In its original formulation, MCEv1 was capable of converging multiple different regimes for varying timeframes in agreement with the MCTDH used as a benchmark. The SBM parameters can be described as follows: Δ is the tunneling parameter (which is often, as in the case here, also used as a scaling parameter); ω_c is the characteristic frequency of the bath; α_k is the Kondo parameter, which describes the coupling between the system and the bath; ε is the energy shift between the minimum energy of the two different potential energy surface; and β is the inverse temperature parameter, given by $\frac{1}{kT}$. The spectral density attached to the spin-boson model is the Ohmic bath, and as such, the lower frequencies increase linearly until the characteristic frequency
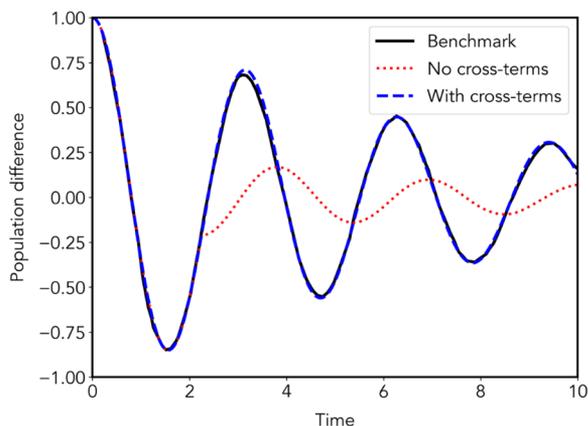
FIG. 7. Symmetrical well spin-boson case with $\omega_c = 2.5$, $\beta = 5$, and $\alpha_k = 0.09$. Comparison of MCEv1 cloned propagations with (dashed) and without (dotted) the inclusion of cross terms to the MCTDH benchmark (solid line). Both MCEv1 propagations performed with $N_{bf} = 50$ basis functions and M = 50 bath modes and converged with 64 repeats or randomly selected "bits."
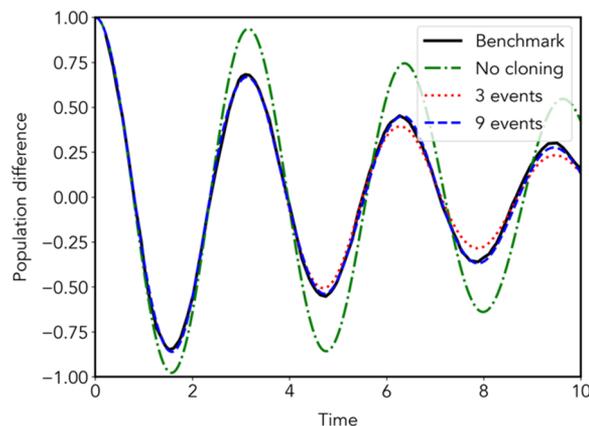

FIG. 8. Symmetrical well spin-boson case with $\omega_c = 2.5$, $\beta = 5$, and $\alpha_k = 0.09$. Comparison of MCEv1 cloned propagations with three cloning events (dotted), nine cloning events (dashed) and without (dotted-dashed) cloning to the MCTDH benchmark (solid line). All MCEv1 propagations were performed with $N_{bf} = 1$ basis function and M = 50 bath modes and converged with 64 repeated randomly selected "bits."

ω_c is reached, where the spectral density then decays exponentially. This information combined with the number of basis functions and bath modes used to discretize SBM spectrum methods is sufficient to detail all spin-boson cases and MCE results presented in this paper. For all cases in this paper, the results are taken to be converged when increasing of any parameter (or decreasing of the time step) does not result in a change of population difference.

The first spin-boson case discussed in this paper is a "simple" case consisting of low-but nonzero temperature symmetrical wells that were previously converged by MCEv1 in its initial paper. As the case is easy to converge, it serves as a great initial demonstration for the application and technicalities of cloning.

Figure 7 demonstrates the necessity of the inclusion of the cross terms between the separately propagating clones of FC-MCEv1. As the clones in full cloning can be regarded as coupled repeats, without the inclusion of cross terms, the two clones created can essentially be seen as restarting propagation from the initial population conditions with misplaced coherent states albeit with opposite starting states, as the clones contain no contribution from one of the potential energy surfaces, similar to their initial conditions. Therefore, as the potential energy wells, in this case, are symmetrical, the propagation of the two clones follows an opposite path and as such the population transfer of each clone cancels out when recombined, producing a flattening of the overall population difference. The remaining muted oscillations occur due to the population imbalance at the time of cloning, so the recombination is not a complete annihilation of the oscillations generated by propagation in this case. Thus, without cross terms, the populations after full cloning are incorrect despite the fact that their sum is equal to one. After the inclusion of the cross terms and the appropriate rescaling of the population, the recombination of the clones is shifted and reproduces a valid population difference.

MCEv1 requires a basis set of 50 basis functions and 50 bath modes to converge to the benchmark, an average computational time per "bit" repeat of 48.54 s. Without cloning, a singular basis function still roughly follows the timing of the oscillations of the benchmark, but greatly overestimates their intensity, even in the shortest timeframe. Figure 8 shows that FC-MCEv1 can match the benchmark with just 1 singular basis function while maintaining the same number of degrees of freedom as the converged result, and the timeframe for which this agreement persists can be increased via increasing the number of cloning events.

With only three cloning events, FC-MCEv1 agrees with the benchmark for more oscillations before slightly diverging. However, the propagation is still fairly accurate for the whole propagation. This is achieved with only three cloning events, all occurring within the first 0.6 atomic time units, essentially having an overall combined basis size of eight basis functions per repeat and 28 total cross terms. Computationally, this costs a fraction of the previous MCEv1 result with 50 basis functions without cloning with an averaging time per "bit" of 1.75 s, greatly decreasing the computational time needed.

For the propagation with nine cloning events, the FC-MCEv1 result is practically exact when compared to the benchmark, fully showing the flexibility of the cloning method. See Fig. 8. However, this large number of cloning events is excessive and introduces its own scaling problem as the final propagation consists of 512 clones and over 250 000 cross terms, with the additional cloning events being at 0.8, 3.7, 4.5, 5.5, 8, and 9 a.u. The computational cost of this propagation is still cheaper that of the full basis set consisting of 50 basis functions, with an average time per "bit" repeat of 36.6 s. Therefore, for the optimization of harder-to-converge cases, there will be sensible balance between the number of cloning events and basis set size. It is also important to note that as the two clones created are propagated separately, the computational cost for cloning in MCEv1 is not identical to that of cloning in MCEv2, with two basis sets of 50 basis functions being cheaper to propagate than one larger basis set of 100 basis functions. This is because the computational cost of propagation scales roughly $\left(N_{bf}\right)^3$. The cross terms are an additional cost but not required at the time of propagation and in

the future can be easily highly parallelized during post-processing. 64 "bit" repetitions were required for convergence.

A. Convergence of MCEv1 and MCEv2 at zero-temperature

Within the zero-temperature regime of the spin-boson model, the MCE methods converge quicker and more accurately to the benchmark when the system has both a low characteristic frequency and a low Kondo parameter. Cases with low coupling have a great number of oscillations before settling to an equilibrium population difference (which is 0, presuming that the wells are symmetrical). As this coupling increases, the oscillations lessen in both frequency and intensity. Within the MCE methods, the easiest case considered would be therefore the case containing both features, in this case $\omega_c = 10$ and $\alpha_k = 0.05$.

Due to the number of oscillations in Fig. 9, the time step required for both MCEv1 and versions of MCEv2 is 0.02, for a total of 2000 time steps. For MCEv2, the initial propagation matches the timing of the oscillations while overestimating their strength and the overall "character" is maintained throughout propagation; however, even the timing of oscillations is quickly lost. With a smaller initial basis set of 100 basis functions and no more than four multiple cloning events per initial basis function, this can be greatly corrected with MC-MCEv2 such that the initial oscillations are practically exact and the mismatch in timing occurs when oscillations are small as the system approaches population equilibrium. More cloning events would lead to agreement at longer times; however, the increase in computational cost will be great as after four cloning events of each initial basis function MC-MCEv2 requires propagation of 1600 basis functions, and allowing an additional cloning event will double the size of the final basis set, making this option computationally infeasible.

For the same case, MCEv1 converges very well with a relatively small basis set, using just 200 basis functions and 200 bath modes. The agreement with the benchmark also persists for longer than that

of the MC-MCEV2 without a need to increase the basis set further. See Fig. 9. The average CPU time per "bit" repeat required for the MCEv1 and the MCEv2 propagation in Fig. 9 is 0.795 and 0.888 CPU hours, respectively, with both methods using a time step of 0.02, showing that while the computational cost is comparable and the basis set size is identical, MCEv1 produces a much more accurate result when compared to the MCTDH benchmark. Once multiple cloning is allowed, MC-MCEv2 presents a significant increase in computational cost with an average CPU time per "bit" repeat of 47.29 CPU hours. This is because between 87 and 95 basis functions clone on the very first time step and by four atomic time units, the basis has increased to 1600 basis functions. 64 "bit" repetitions were required for convergence for both MCEv1 and MCEv2.

Increasing the coupling between the system and the bath via the Kondo parameter has the effect of reducing the number and strength of the oscillations, although the same time step of 0.02 is still applied. Slightly increasing the coupling strength to $\alpha_k = 0.1$ is sufficient of a difference that MCEv2 becomes less qualitative with more rapid mistiming of the oscillations and the introduction of a distortion of the overall dampening of oscillations to the equilibrium population difference. With the introduction of four cloning events per each initial basis function, MC-MCEv2 with a final basis size of 1600 basis functions now correctly simulates the behavior of the system but consistently slightly underestimates the strength of the oscillations. Similar to the previous case considered, the cloning events in MCEv2 are entirely contained within the first four atomic time units and the vast majority of basis functions have their first cloning event on the first time step, with the computational time increasing again to 46.2 CPU hours from the 0.788 CPU hours per "bit" repeat required for MCEv2 without trains or cloning.

MCEv1 is once again capable of converging to the accuracy of the benchmark with the same-sized basis set and without any full cloning events, with an average computational cost of 0.775 CPU hours per "bit" repeat (see Fig. 10). 64 "bit" repetitions were required for convergence for both MCEv1 and MCEv2.
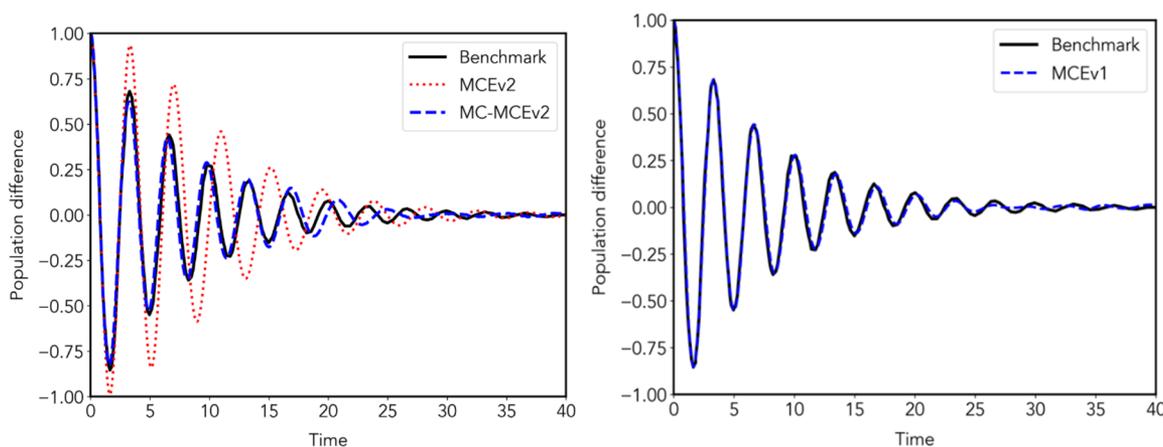

FIG. 9. Symmetrical well spin-boson case with $\omega_c = 10$, $\beta = 5000$ (as an estimation of infinity), and $\alpha_k = 0.05$. MCEv1 (right, dashed), MCEv2 (left, dotted), and MC-MCEv2 (left, dashed) were all compared to the MCTDH benchmark (solid line). MCEv1 and MCEv2 parameters: $N_{bf} = 200$ basis functions and $M = 200$ bath modes. MC-MCEv2 parameters: $N_{bf} = 100$ initial basis functions and $M = 200$ bath modes. All runs converged with 64 repeats or randomly selected "bits."
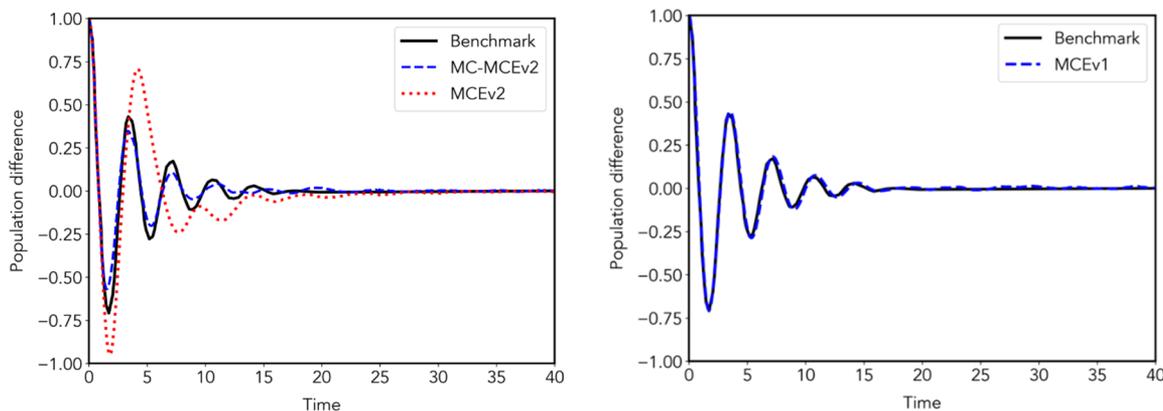
30 August 2024 10:51:38

FIG. 10. Symmetrical well spin-boson case with $\omega_c = 10$, $\beta = 5000$ (as an estimation of infinity), and $\alpha_k = 0.1$. MCEv1 (right, dashed line), MCEv2 (left, dotted line), and MC-MCEv2 (left, dashed line) were all compared to the MCTDH benchmark (solid line). MCEv1 and MCEv2 parameters: $N_{bf} = 200$ basis functions and $M = 200$ bath modes. MC-MCEv2 parameters: $N_{bf} = 100$ initial basis functions and $M = 200$ bath modes. All runs converged with 64 repeats or randomly selected "bits."

As the coupling strength increases, it becomes less common for MCEv1 to be capable of converging perfectly. Moving from the regime of weak coupling to that of moderate strength requires the introduction of cloning while utilizing the other sampling techniques of swarms and the search for the optimal compression parameter. For the case with $\alpha_k = 0.4$, the initial rate of population transfer from state 1 to state 2 is correct; however, the propagation slowly drifts away from the equilibrium population difference, at late times. With a singular angular full cloning event, FC-MCEv1 can retain the small size of the basis set size with just 200 basis functions and 100 bath modes while better matching the benchmark. The number of time steps per unit time can be reduced when the propagation no longer contains a large number of close oscillations,

resulting in a time step of 0.05. The angular cloning event occurs when the population difference approaches zero from below, and most of the cloning events occur around time step 105 of 300. Introduction of these cloning events increases the computational time for the whole run from 4.62 CPU minutes to 7.88 CPU minutes per "bit" repeat. Despite the fact that full wave function cloning doubles the number of basis functions, the computational time has not doubled. This is due to the clones not being propagated as one doubled basis but instead can be seen as propagating an additional coupled bit repeat. It is important to note that the times given are per core and so would only be equal to the elapsed time for the whole propagation if the clones were propagated one after the other. Since the cloned basis sets can be run independently in parallel, the true
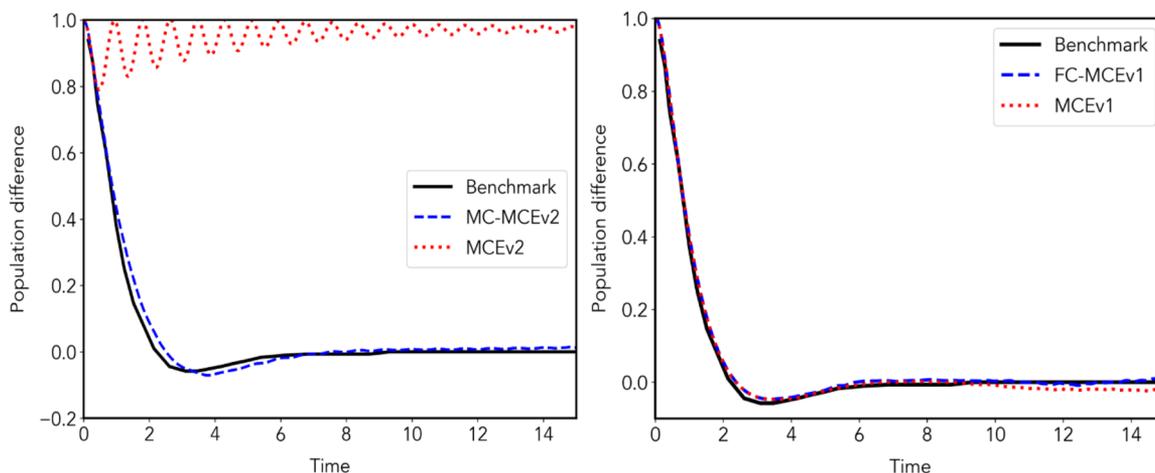

FIG. 11. Symmetrical well spin-boson case with $\omega_c = 10$, $\beta = 5000$ (as an estimation of infinity), and $\alpha_k = 0.4$. MCEv1 (right, dotted), FC-MCEv1 (right, dashed), MCEv2 (left, dotted), and MC-MCEv2 (left, dashed) were all compared to the MCTDH benchmark (solid line). MCEv1 and MCEv2 parameters: $N_{bf} = 200$ basis functions and $M = 200$ bath modes. MC-MCEv2 parameters: $N_{bf} = 100$ initial basis functions and $M = 200$ bath modes. FC-MCEv1 parameters: $N_{bf} = 200$ basis functions and $M = 100$ bath modes. All runs converged with 64 repeats or randomly selected "bits."

elapsed time per "bit" repeat has the potential to be lower. In the case of MCEv2, this case demonstrates the strength of the different sampling methods that construct MC-MCEv2 as while the method is capable of converging relatively close to the benchmark, without these tools MCEv2 is trapped in tiny oscillations starting at the beginning of propagation, completely unrecognizable to the benchmark result. While MCEv2 without cloning is not viable for this scenario, it can be used on the same increased time step as MCEv1 and so reported an average computational time per "bit" repeat of 4.62 CPU minutes. However, this advantageous time step cannot be used in MC-MCEv2 as a smaller time step is required for the formation of trains, returning to the time step of 0.02. This combined with the limit of the four cloning events allowed significantly increases the time per "bit" repeat to 10.7 CPU hours. The MC-MCEv2 propagation begins propagation with 100 basis functions, but between 40 and 60 extra basis functions are created on the first time step, and by eight atomic time units, the final basis set size of 1400–1550 basis functions has been reached. See Fig. 11. 64 "bit" repetitions were required for convergence for both MCEv1 and MCEv2.

For a case within the moderate coupling strength regime such as that of $\alpha_k = 0.55$, it is apparent that while MC-MCEv2 is a great improvement on standard MCEv2, the method is not able to capture the full decay to equilibrium population difference. However, the sampling tricks again transform the result from unrecognizable to semi-quantitatively correct. This is because even after the time step is reduced to 0.012 in order to properly form the trains of the initial basis set, each basis function only clones at most once, and all cloning events occur before 2.5 atomic time units resulting in a final average computational time of 0.643 CPU hours per "bit" repeat. The sampling tricks of MC-MCEv2 increase the cost of the propagation but as Fig. 12 a single cloning event and trains can significantly improve the result. Allowing the propagation to therefore start with a smaller initial basis set can be economical with the MC-MCEv2 propagation taking less computational power than the MCEv2

propagation with an average computational time of 0.911 CPU hours per "bit" repeat when propagated with the larger basis set of 200 basis functions and 200 bath modes. Zero-temperature cases were previously noted as limiting cases for MC-MCEv2,[40] and it can be concluded that the coupling strength limit for MC-MCEv2 at this characteristic frequency has now been reached.

When looking at MCEv1 in this scenario, the decay of population from state 1 is accurately captured but MCEv1 misestimates the final population and as such the decay persists for longer than the benchmark. Similarly with MC-MCEv2, the disagreement with the benchmark at later times is larger for the cases with stronger couplings. If full cloning is applied here, a singular cloning event is enough to correct this final population, and FC-MCEv1 can be converged to the benchmark with a fairly low number of basis functions, with a basis set size of merely 50 basis functions attached to 200 bath modes. This cloning event causes a minimal increase in computational cost from an average of 2.28–2.69 CPU minutes per "bit" repeat. This small increase is due to a portion of CPU time spent generating the initial basis which is completely identical whether cloning will be used later in propagation or not. Another large factor is that as MCEv1 requires multiple repeats in order to average to the correct result, each repeat clones at a different time step, with most cloning events in this case considered in Fig. 12 ranging from time 7 to 22.5 a.u., with the latest cloning time of 39.8 atomic time and ten repeats that had no cloning event throughout the whole propagation. See Fig. 12.

The strong to ultra-strong coupling regime can present a difficult challenge to the MCE methods due to the large number of basis functions and bath modes required for convergence. MCEv1 in its original paper was shown to converge to an ultra-strong coupling of $\alpha_k = 1.5$ for the different characteristic frequencies of $\omega_c = 10$, 20 and 40 for a short timeframe. For each characteristic frequency, there is a value for the Kondo parameter for which the propagation will not relax to a negligible population difference within 40 atomic
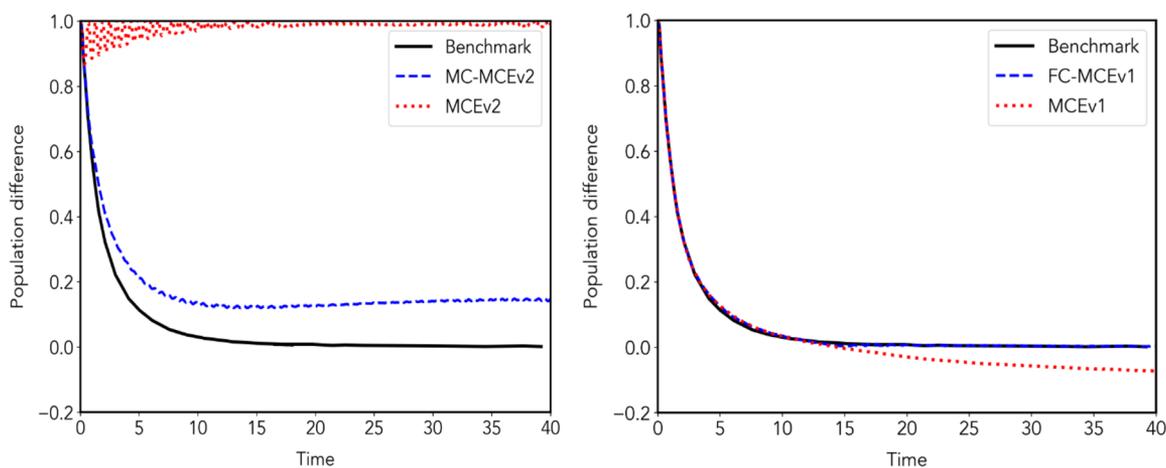
FIG. 12. Symmetrical well spin-boson case with $\omega_c = 10$, $\beta = 5000$ (as an estimation of infinity), and $\alpha_k = 0.55$. MCEv1 (right, dotted), FC-MCEv1 (right, dashed), MCEv2 (left, dotted), and MC-MCEv2 (left, dashed) were all compared to the MCTDH benchmark (solid line). MCEv1 and FC-MCEv1 parameters: $N_{bf} = 50$ basis functions and $M = 200$ bath modes. MCEv2 parameters: $N_{bf} = 200$ basis functions and $M = 200$ bath modes. MC-MCEv2 parameters: $N_{bf} = 100$ initial basis functions and $M = 200$ bath modes. All runs converged with 64 repeats or randomly selected "bits."
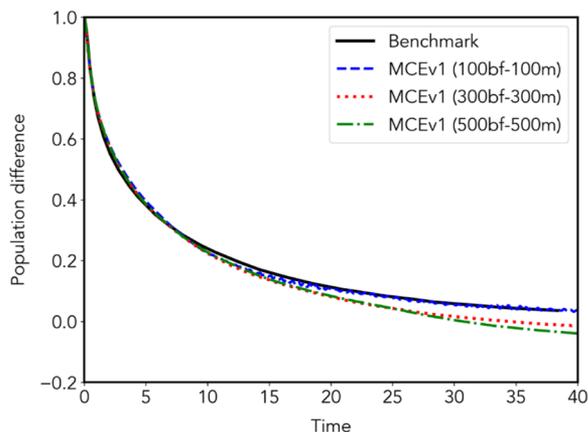
FIG. 13. Symmetrical well spin-boson case with $\omega_c = 20$, $\beta = 5000$ (as an estimation of infinity), and $\alpha_k = 0.4$. MCEv1 (right) shows propagation without cloning for different basis set sizes, compared to the MCTDH benchmark (solid line). All runs converged with 64 repeats or randomly selected "bits."

time units, the longest timeframe studied in this paper, meaning that in the strong coupling regime, a cloning scheme based on population difference would not be suitable. Therefore, while several strong coupling regime scenarios can be converged with MCEv1 without cloning, a more generalized cloning condition than a population difference of 0 will have to be derived to apply FC-MCEv1 converge the cases that are currently inaccessible for other MCE methods.

Figure 13 displays a sensitivity to the MCEv1 method in that surprisingly the smallest basis set converges closest to the MCTDH benchmark, without the need for cloning. This phenomenon is not as contradictory as it seems at first glance as the increase in basis set size follows the increase in the number of bath modes, which can in turn demand an even larger number of basis functions. This growth

in required basis functions is not guaranteed to be linear and so the larger basis functions cannot be considered fully converged internally within MCEv1, i.e., converged to the number of repeats, but not to the number of basis functions. A certain care must be taken therefore when increasing both the number of modes in SBM discretization and the basis set size to ensure convergence of all basis set parameters. The computational time for the MCEv1 results considered in Fig. 13 also demonstrates the advantage of basis set growth at pivotal points of propagation instead of propagating a larger basis set for the entire timeframe. The smallest basis set of 100 basis functions and 100 bath modes requires only an average of 3.56 CPU minutes per "bit" repeat, whereas the medium basis set of 300 basis functions and 300 bath modes requires and an average of 1.16 CPU hours per "bit" repeat. The cost of increasing the basis set by another 200 basis functions and bath modes essentially quintuples as the MCEv1 propagation with 500 basis functions and 500 bath modes requires an average of 5 CPU hours of computational time per "bit" repeat. 64 "bit" repetitions were required for all MCEv1 results for convergence.

With an increase in characteristic frequency to $\omega_c = 20$ and a return to the weak coupling regime, MCEv1 is once again capable of converging exactly to the benchmark of MCTDH without the need for any cloning events. As MCEv1 can match the MCTDH benchmark of this increased characteristic frequency without a need to increase the basis set, the computational cost required is roughly equal to that of Figs. 9 and 10 with an average "bit" repeat time of 0.73 CPU hours. MCEv2 can also produce better results once again in the weaker coupling cases although due to increased characteristic frequency, the deformation of the oscillations occurs more readily and more often, even in the weakest case studied with $\alpha_k = 0.05$, cloned swarms of trains are required to maintain full oscillations. MC-MCEv2 is still unable to converge correctly after four cloning events in this case, matching the initial oscillations within the region of cloning before too quickly settling to the equilibrium, where additional cloning events would be required. The MCEv2 and
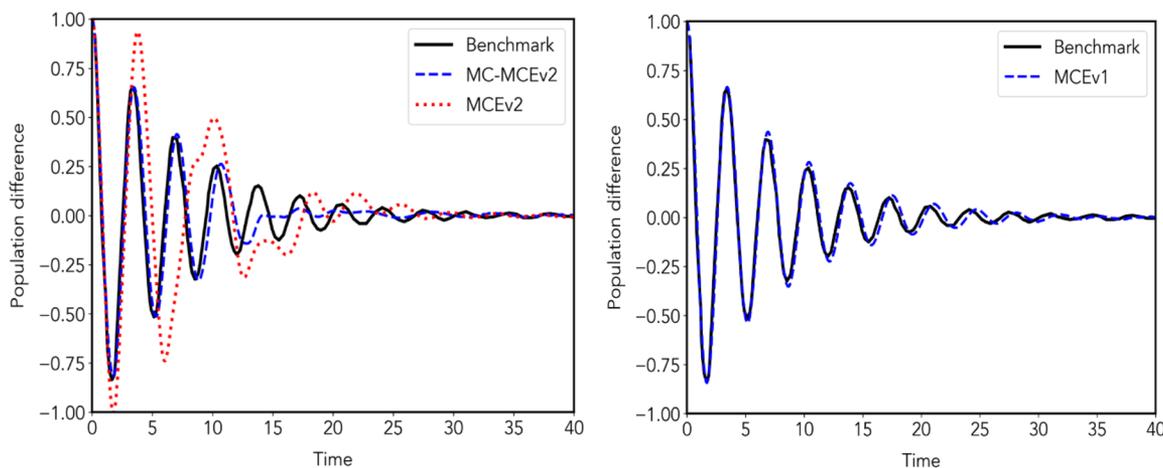

FIG. 14. Symmetrical well spin-boson case with $\omega_c = 20$, $\beta = 5000$ (as an estimation of infinity), and $\alpha_k = 0.05$. MCEv1 (right, dashed), MCEv2 (left, dotted), and MC-MCEv2 (left, dashed) were all compared to the MCTDH benchmark (solid line). MCEv1 and MCEv2 parameters: $N_{bf} = 200$ basis functions and $M = 200$ bath modes. MC-MCEv2 parameters $N_{bf} = 100$ initial basis functions and $M = 200$ bath modes. All runs converged with 64 repeats or randomly selected "bits."
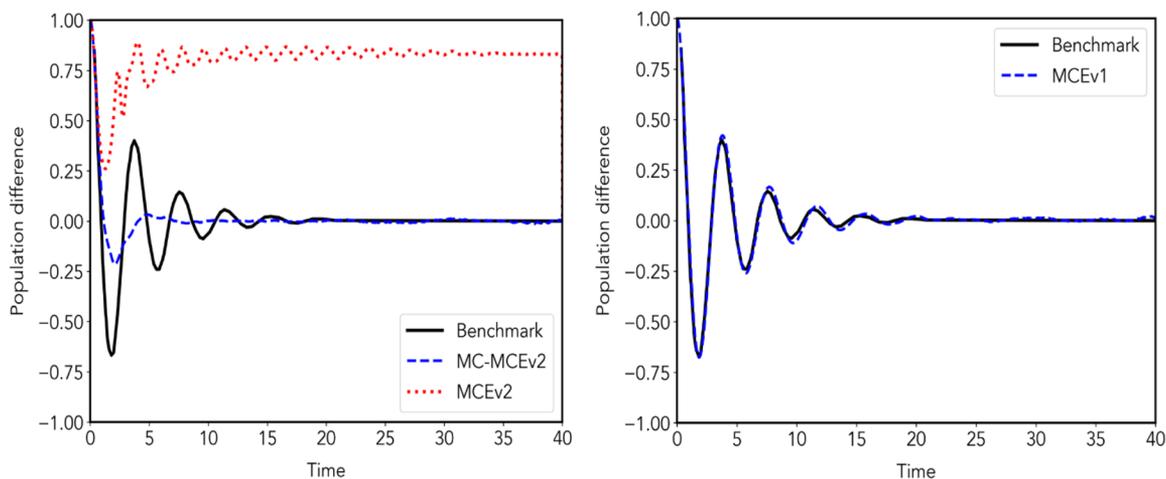
FIG. 15. Symmetrical well spin-boson case with $\omega_c = 20$, $\beta = 5000$ (as an estimation of infinity), and $\alpha_k = 0.1$. MCEv1 (right, dashed), MCEv2 (left, dotted), and MC-MCEv2 (left, dashed) were all compared to the MCTDH benchmark (solid line). MCEv1 and MCEv2 parameters: $N_{bf} = 200$ basis functions and $M = 200$ bath modes. MC-MCEv2 parameters $N_{bf} = 100$ initial basis functions and $M = 200$ bath modes. All runs converged with 64 repeats or randomly selected "bits."

MC-MCEv2 results shown also have similar averaged computational times to previous cases of 0.962 and 47.06 CPU hours per "bit" repeat respectively, with the cloning in MCEv2 taking on the "usual" behavior for these zero-temperature cases. See Fig. 14. 64 "bit" repetitions were required for convergence for both MCEv1 and MCEv2.

With the increased characteristic frequency, MCEv2 quickly returns to the behavior of high-frequency oscillations where the population is trapped on the first state at the weak coupling strength of $\alpha_k = 0.1$, with an average computational time of 0.974 CPU hours per "bit" repeat. This is also the first case for MC-MCEv2 that it fails to capture at least the qualitative behavior as no oscillations are present, although it does converge to the correct final population

difference, despite the four cloning events occurring and the average computational time per "bit" repeat increasing to 46.42 CPU hours. MCEv1 performs similarly to the previous case in that it still can converge accurately and quickly to the benchmark without any need for cloning, with an average computational time of 0.73 CPU hours per "bit" repeat. See Fig. 15. 64 "bit" repetitions were required for convergence for both MCEv1 and MCEv2.

Figure 16 shows that for MCEv1 $\alpha_k = 0.4$ once again acts as the threshold for when cloning is necessary for the method to converge with a reasonably sized basis set. With the increase of the characteristic frequency, the time spent with a negative population difference extends while the magnitude of the most negative population dif-
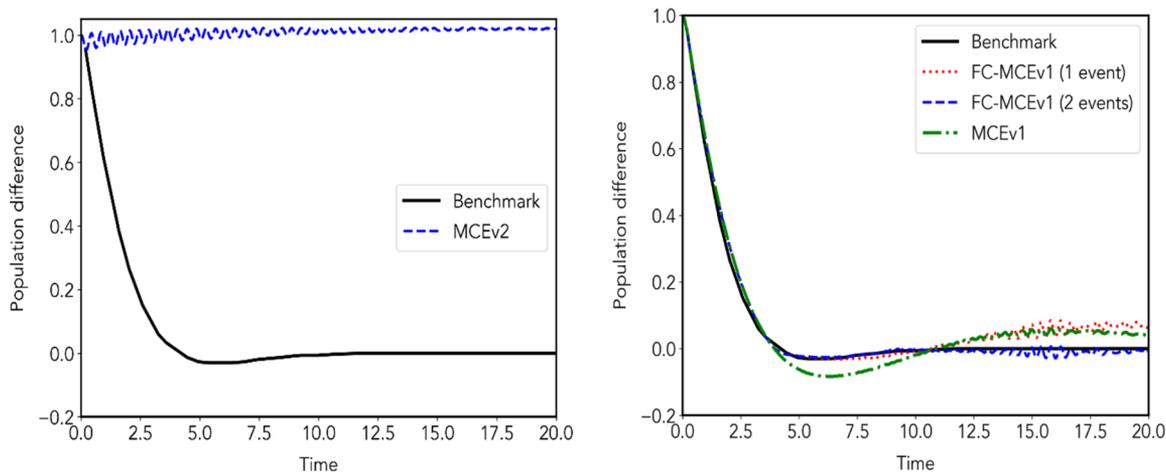

FIG. 16. Symmetrical well spin-boson case with $\omega_c = 20$, $\beta = 5000$ (as an estimation of infinity), and $\alpha_k = 0.4$. MCEv1 (right, dashed), FC-MCEv1 (right, dotted), and MCEv2 (left, dotted) were all compared to the MCTDH benchmark (solid line). MCEv1 and FC-MCEv1 parameters: $N_{bf} = 200$ basis functions and $M = 100$ bath modes. MCEv2 parameters: $N_{bf} = 200$ basis functions and $M = 200$ bath modes. All runs converged with 64 repeats or randomly selected "bits."

ference decreases. Despite the lack of oscillations, the increased characteristic frequency prohibits larger time steps and so the time step remains 0.02. MCEv1 is capable of matching the initial population descent but moves away from the benchmark after crossing into negative population difference and mistakenly introduces very weak and wide oscillations. With a single cloning event, FC-MCEv1 continues to match the benchmark for longer before eventually, the population begins to transfer to state 1 and follow closer to the original MCEv1 propagation without cloning. However, with two cloning events, the converged result follows significantly closer to the benchmark for much longer, with a basis set size of 200 basis functions and 100 bath modes. The cloning condition for this case was the overall population difference reached 0. Figure 16 encapsulates the increasing cost of full cloning. The FC-MCEv1 propagation with only one cloning event increased the average computational time from 0.244 to 0.394 CPU hours per "bit" repeat. This cloning event occurred very consistently across the repetitions with almost all events occurring between 3.7 and 4.2 atomic time units. The second cloning event is also fairly consistent with almost all second cloning events occurring between 8.4 and 10.2 atomic time units and introducing the second cloning event increases the computational cost to 0.84 CPU hours per "bit" repeat. This is because after the second cloning event, FC-MCEv1 requires propagation of four clones along with six sets of cross terms. For MCEv2, the method struggles to generate a correct train-spacing parameter without severely decreasing the time step and therefore inversely increasing the computational time causing the train technique to be unfeasible. Cloning within this case also becomes near impossible as without a sufficiently spaced train, no basis functions reach even a lowered condition for cloning and so without cloning events or train spacing, MCEv2 and MC-MCEv2 become identical and therefore $\alpha_k = 0.4$ can be described as a limit of the MC-MCEv2 method for $\omega_c = 20$. 64 "bit" repetitions were required for convergence for both MCEv1 and MCEv2.

Similar to the previous case presented in Fig. 12 cloning is required when the Kondo parameter, α_k, is increased to 0.5 in Fig. 17. However, unlike the previous case, the higher characteristic frequency results in the propagation diverging from the benchmark before the population difference reaches 0. For FC-MCEv1 to match the MCTDH benchmark, it is necessary to enact full cloning events of both forms described in Eqs. (17) and (18). A slight deviation in the descent of population difference is corrected by an angular full cloning event [Eq. (19)] when the population difference is 0.1. Then in order to maintain the equilibrium population difference, a standard full cloning event occurs when there is 0-population difference, as with other cases presented in this article. This divergence from our normal cloning condition highlights the need for a more automatic acknowledgment of when cloning is needed. For all cases, a sufficiently large basis set of MCEv1 will be accurate for short times. However, the strength of MCEv1 lies with its coupled Ehrenfest trajectories and as propagation continues, these trajectories slowly uncouple explaining why MCEv1 struggles more with cases with higher dimensionality or stronger coupling as this decoupling process happens more readily. This case shows that for difficult cases it is possible to converge to a benchmark via increasing the number of cloning events instead of increasing the basis set size and as such the basis set size for this case remains small with 50 basis functions and 200 bath modes. FC-MCEv1 is also economical as the average computational cost is 4.81 CPU minutes per "bit" repeat, compared
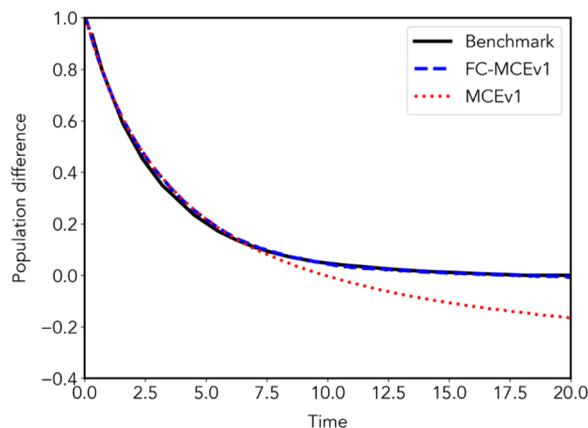

FIG. 17. Symmetrical well spin-boson case with $\omega_c = 20$, $\beta = 5000$ (as an estimation of infinity), and $\alpha_k = 0.5$. MCEv1 (dashed), FC-MCEv1 was compared to the MCTDH benchmark (solid line). Both MCEv1 propagations had the following parameters: 50 basis functions and 200 bath modes. All runs converged with 64 repeats or randomly selected "bits."

to 2.81 CPU minutes for an MCEv1 propagation without cloning. The reason for the smaller increase in computational time compared with Fig. 16 is while the propagation allowed for two cloning events and every "bit" repeat had an initial cloning event, only 86 of the 128 clones created initiated the cloning procedure again, with the time of second cloning widely ranging from 6.5 to 17.5, there were also repetitions who did not undergo the first angular cloning event until late into propagation, with the latest angular cloning event occurring at 16.4 atomic time units, with more common angular cloning events in the range of 6–11. See Fig. 17.

$\omega_c = 40$ is the largest characteristic frequency studied in this paper and presents a significant challenge to the MCE methods due to the computational cost required. This increase in cost from lower characteristic frequencies is twofold, the most obvious is that cases with larger characteristic frequencies require more degrees of freedom in order to properly converge, and so the required basis sets are larger. The second is that of the viable time step. As the characteristic frequency increases, the smaller the time steps required to maintain the stability of MCE equations of motion. In practice, the largest viable time step for a case with $\omega_c = 40$ is ~4 times smaller than the largest time step in the $\omega_c = 10$ cases. 64 "bit" repetitions were required for convergence.

The increase in bath modes required to discretize the spectrum of SBM in Fig. 18 is a direct result of the increase in characteristic frequency. MCEv1 is still capable of matching the benchmark, with a slight disagreement increasing every oscillation. However, even at late times, the difference between MCEv1 and the MCTDH benchmark is not large, and the propagation is quantitative for all times. Due to the high characteristic frequency of this case, the time step has to be reduced to 0.01 and 4000 total time steps are required and the computational cost is 2.61 CPU hours per "bit" repeat. 64 "bit" repetitions were required for convergence. This is the weakest coupling case, and the subsequent increase in the coupling strength dramatically increases the number of modes required, with cases in the moderate coupling regime for $\omega_c = 40$ requiring up to 1000 s
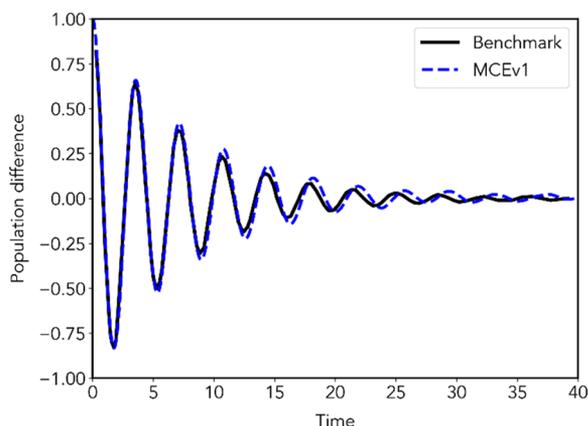
FIG. 18. Symmetrical well spin-boson case with $\omega_c = 40$, $\beta = 5000$ (as an estimation of infinity), and $\alpha_k = 0.05$. MCEv1 (dashed) was compared to the MCTDH benchmark (solid line). MCEv1 parameters: $N_{bf} = 200$ basis functions and $M = 300$ bath modes. All runs converged with 64 repeats or randomly selected "bits."

of modes, increasing significantly further the CPU times. We are working on the convergence of this most computationally demanding case; however, it is clear that further enhancements to the full cloning procedure will be necessary to address this challenge, for instance by introducing more flexible cloning conditions. Therefore, a further study into the coupling strength limit of FC-MCEv1 will be performed after said condition is established.

VI. CONCLUSIONS AND DISCUSSIONS

The zero-temperature spin-boson regime was explored through the lens of both MCEv1 and MCEv2. The coupling limit for each characteristic frequency for the MCEv2 was discovered, showing where the computational tricks such as trains and cloning begin to break down. MCEv1 was shown to be capable of converging to the MCTDH benchmark for more cases than MCEv2. During several cases considered in this paper, it was noted that even with a lowered cloning condition, MC-MCEv2 had a significant portion of its basis function clone at the same time step. This could suggest that a full cloning approach to cloning in MCEv2 could be economical and may be beneficial in the convergence of these difficult cases. The formal introduction of the cloning sampling technique was implemented into multiconfigurational Ehrenfest version 1 and was proven to be a valuable tool in the convergence of several additional cases. Due to the lack of a flexible full cloning parameter, the results presented are considered preliminary "proof-of-concept" results and future work will involve converging more zero-temperature cases with higher characteristic frequency and other regimes of SBM. Cloning in MCEv1 has the potential to be cheaper than the version present in MCEv2 in situations where a large percentage of the basis functions need to be cloned as propagating two parallel basis sets separately is computationally cheaper than propagating a basis that has doubled in size. Theoretically, the greatest limiting factor for excessive cloning events in MCEv1 is in the interacting cross terms. However, it is also important to note that the computational times provided are given per CPU core as each "bit" repeat occupies

one core, and in practice, the different repeats are run in parallel. This parallelization could be taken further by running the basis sets created after a full cloning event in parallel, further reducing real time computational cost compared to the cloning in MC-MCEv2. In practice, however, the current greatest limit of FC-MCEv1 is the lack of an automatic cloning parameter that can be used so that the method itself can recognize when cloning is required without user input. In almost all cases here, we have done cloning at the point of equal population of the two electronic states, but a systematic study of other potential full cloning conditions is required. The general process for converging a result from the MCE methods is as follows: first, the number of "bit-by-bit" repetitions and the time step can be considered trivial to converge. Then, the basis set size is increased and finally the number of cloning events. Therefore, the development of such a procedure is a vital step of the future development of the method and will be derived after a systematic review of full cloning across many cases.

The increased characteristic frequency and therefore the required dimensions to converge the result as α_k increases beyond very weak coupling has been prohibitive to continuous testing of the full cloning procedure on further $\omega_c = 40$ cases. An issue was also encountered where a cloning event could be required after sufficient propagation time, and therefore, the trajectories that guide the initial basis set would have traveled sufficiently that the Ehrenfest configurations and trajectories could be taken to be uncoupled. If this happens and a full cloning event occurs, the newly generated basis sets will continue to be uncoupled and therefore will not be faithful to the system they are attempting to represent. This suggests that full cloning for cases for systems with very high dimensionality or cases that require cloning at late times may also require resampling to reestablish coupling. The nature of this procedure will be investigated as future work.

There is also interest in exploring more regimes that are yet to be studied with the MCE methods. Most MCE papers have centralized on the exponential cutoff applied to the Ohmic spectral density, but there are a multitude of different methods that investigate sub and super-Ohmic cases with spectral density with a Drude Lorentzian cutoff, often studied by the hierarchical equations of motion.[18–20] A more generally applicable full cloning MCEv1 should be capable of converging high dimensionality cases with relatively small basis sets such as the case shown in Fig. 17.

While for the moment the coupled trajectories of MCEv1 make its application to *ab initio* "on-the-fly" dynamics difficult, with some effort, it may be used in the future for direct dynamics. The vMCG community has recently presented developments of such an *ab initio* extension of their method.[59] A comparable effort could be made to construct an extension for MCEv1, and the Ehrenfest trajectories that guide the basis set would be computationally advantageous, due to avoiding the complexity and instabilities of variational trajectories. However, now, it is an efficient method for simulating systems where the potential energy surfaces are well known. The method is well suited to future applications in the study of biological molecules where potential energy surfaces are commonly found by "spin-boson-like" models such as the linear vibronic coupling[60,61] model, and recently, extensions have been made to the MCEv1 method to study the Holstein polaron[44] and to simulate time- and frequency-resolved four-wave-mixing signals.[62] The quantum dynamics for these molecules are often performed with multi-layer MCTDH,[23]

but hopefully, MCEv1 also becomes a useful tool. The choice of potential methods to tackle these problems is limited as the high dimensionality required often out scales the viability of most quantum dynamic methods. Our hope is that with a more generalized full cloning, MCEv1 could join the list of potential methods for these molecules. MCEv2 has already proved to be a useful method for non-adiabatic molecular dynamics with the AIMC-MCE approach.[55] The current work reinforces the understanding of MCEv2 convergence properties and shows that with the right sampling, it is capable of delivering good results in complicated zero-temperature quantum regimes.

ACKNOWLEDGMENTS

AUTHOR DECLARATIONS

Conflict of Interest

The authors have no conflicts to disclose.

Author Contributions

Ryan Brook: Conceptualization (equal); Data curation (equal); Formal analysis (equal); Investigation (equal); Methodology (equal); Software (equal); Validation (equal); Visualization (equal); Writing – original draft (equal); Writing – review & editing (equal). **Christopher Symonds**: Conceptualization (equal); Methodology (equal); Software (equal). **Dmitrii V. Shalashilin**: Conceptualization (equal); Methodology (equal); Supervision (equal); Writing – original draft (equal); Writing – review & editing (equal).

DATA AVAILABILITY

The data are available upon reasonable request. The repository for code used to simulate the results of this paper can be found in our research group GitHub: https://github.com/CompChemLeeds/MCE.

REFERENCES

[1] A. J. Leggett *et al.*, Rev. Mod. Phys. **59**, 1 (1987).
[2] A. Lemmer *et al.*, New J. Phys. **20**, 073002 (2018).
[3] R. Puebla *et al.*, Symmetry **11**, 695 (2019).
[4] P. J. Ollitrault, G. Mazzola, and I. Tavernelli, Phys. Rev. Lett. **125**, 260511 (2020).
[5] D. Xu and K. Schulten, Chem. Phys. **182**, 91 (1994).
[6] B. Jaderberg *et al.*, New J. Phys. **24**, 093017 (2022).
[7] U. Weiss, H. Grabert, and S. Linkwitz, J. Low Temp. Phys. **68**, 213 (1987).
[8] A. Suarez and R. Silbey, J. Chem. Phys. **95**, 9115 (1991).
[9] M. B. Cibils *et al.*, J. Phys. A: Math. Gen. **24**, 1661 (1991).
[10] F. Giraldi and F. Petruccione, Int. J. Quantum Inf. **10**, 1241001 (2012).
[11] V. M. Kenkre and L. Giuggioli, Chem. Phys. **296**, 135 (2004).
[12] D. Mac Kernan, G. Ciccotti, and R. Kapral, J. Chem. Phys. **116**, 2346 (2002).
[13] M. Ben-Nun and T. J. Martinez, Isr. J. Chem. **47**, 75 (2007).
[14] A. Luck *et al.*, Phys. Rev. E **58**, 5565 (1998).
[15] B. Gardas, J. Phys. A: Math. Theor. **44**, 195301 (2011).
[16] Y. Tanimura, J. Chem. Phys. **153**, 020901 (2020).
[17] L. Wang *et al.*, J. Chem. Phys. **146**, 124127 (2017).
[18] C. R. Duan *et al.*, Phys. Rev. B **95**, 214308 (2017).
[19] J. Tang *et al.*, J. Chem. Phys. **143**, 224112 (2015).
[20] C. R. Duan *et al.*, J. Chem. Phys. **147**, 164112 (2017).
[21] H. D. Zhang *et al.*, J. Chem. Phys. **152**, 064107 (2020).
[22] H. D. Meyer, U. Manthe, and L. S. Cederbaum, Chem. Phys. Lett. **165**, 73 (1990).
[23] H. B. Wang and M. Thoss, J. Chem. Phys. **119**, 1289 (2003).
[24] H. B. Wang and M. Thoss, New J. Phys. **10**, 115005 (2008).
[25] H. B. Wang and M. Thoss, Chem. Phys. **370**, 78 (2010).
[26] S. Wenderoth, H. P. Breuer, and M. Thoss, Phys. Rev. A **104**, 012213 (2021).
[27] D. V. Shalashilin, J. Chem. Phys. **130**, 244101 (2009).
[28] D. V. Shalashilin, J. Chem. Phys. **132**, 244111 (2010).
[29] E. J. Heller, J. Chem. Phys. **75**, 2923 (1981).
[30] H. Shore and L. M. Sander, Phys. Rev. B **7**, 4537 (1973).
[31] M. Ben-Nun, J. Quenneville, and T. J. Martinez, J. Phys. Chem. A **104**, 5161 (2000).
[32] M. Ben-Nun and T. J. Martínez, J. Chem. Phys. **112**, 6113 (2000).
[33] B. Mignolet and B. F. E. Curchod, J. Chem. Phys. **148**, 134110 (2018).
[34] B. F. E. Curchod, W. J. Glover, and T. J. Martinez, J. Phys. Chem. A **124**, 6133 (2020).
[35] M. Ronto and D. V. Shalashilin, J. Phys. Chem. A **117**, 6948 (2013).
[36] Y. Zhao *et al.*, Wiley Interdiscip. Rev.: Comput. Mol. Sci. **12**, e1589 (2022).
[37] A. S. Davydov, Phys. Status Solidi B **36**, 211 (1969).
[38] A. Davydov, J. Theor. Biol. **38**(3), 559 (1973).
[39] Y. Toyozawa, Prog. Theor. Phys. **26**, 29 (1961).
[40] Y. Zhao, D. W. Brown, and K. Lindenberg, J. Chem. Phys. **107**, 3159 (1997).
[41] G. Venzl and S. F. Fischer, J. Chem. Phys. **81**, 6090 (1984).
[42] R. Wang and Z. G. Wang, J. Chem. Phys. **144**, 024101 (2016).
[43] L. Chen, M. Gelin, and Y. Zhao, Chem. Phys. **515**, 108 (2018).
[44] L. Chen, M. F. Gelin, and D. V. Shalashilin, J. Chem. Phys. **151**, 244116 (2019).
[45] Y. Zhao, J. Chem. Phys. **158**, 080901 (2023).
[46] V. M. Freixas *et al.*, Phys. Chem. Chem. Phys. **20**, 17762 (2018).
[47] J. A. Green *et al.*, Phys. Chem. Chem. Phys. **21**, 3832 (2019).
[48] D. V. Makhov *et al.*, J. Chem. Phys. **141**, 054110 (2014).
[49] D. V. Makhov *et al.*, Phys. Chem. Chem. Phys. **17**, 3316 (2015).
[50] D. V. Makhov, T. J. Martinez, and D. V. Shalashilin, Faraday Discuss. **194**, 81 (2016).
[51] H. J. Song *et al.*, J. Chem. Theory Comput. **17**, 3629 (2021).
[52] C. C. Symonds *et al.*, Phys. Chem. Chem. Phys. **21**, 9987 (2019).
[53] C. Symonds, J. A. Kattirtzi, and D. V. Shalashilin, J. Chem. Phys. **148**, 184113 (2018).
[54] B. G. Levine *et al.*, Chem. Phys. **347**, 3 (2008).
[55] V. M. Freixas *et al.*, J. Chem. Theory Comput. **19**, 5356 (2023).
[56] D. V. Makhov and D. V. Shalashilin, Chem. Phys. **515**, 46 (2018).
[57] D. V. Shalashilin and M. S. Child, J. Chem. Phys. **128**, 054102 (2008).
[58] S.-Y. Ye, "Coherent effects in dispersive quantum dynamics," Ph.D. thesis (Department of Physics and Astronomy, University College London, 2012).
[59] G. Christopoulou, A. Freibert, and G. A. Worth, J. Chem. Phys. **154**, 124127 (2021).
[60] J. A. Green and R. Improta, Phys. Chem. Chem. Phys. **22**, 5509 (2020).
[61] J. A. Green *et al.*, Molecules **26**, 1743 (2021).
[62] Z. Chen *et al.*, J. Chem. Phys. **154**, 054105 (2021).

30 August 2024 10:51:38